Self-organization of memory activity through spike-timing-dependent plasticity

Katsunori Kitano,[1] Hideyuki Câteau[2] and Tomoki Fukai[1,2,CA]

[1]Department of Information-Communication Engineering, Tamagawa University, 6-1-1 Tamagawagakuen, Machida, Tokyo 194-8610; [2]CREST, JST (Japan Science and Technology), Japan

[CA,1]Corresponding Author and Address

Received 10 January 2002; accepted 15 February 2002

We studied the self-organization of memory-related activity through spike-timing-dependent plasticity (STDP). Relatively short time windows (~10 ms) for the plasticity rule give rise to asynchronous persistent activity of low rates (20–30 Hz), which is typically observed in delay periods of working memory task. We demonstrate some network level effects on the activity regulation that cannot be addressed in single-neuron studies. For longer time windows (~20 ms), the layered cell assemblies that propagate synchronized spikes (synfire chain) are self-organized. Synchronous spike propagation was suggested to underlie the precisely timed spikes in the monkey prefrontal cortex. The present results suggest that the two networks for sustained activity are different realizations of the same principle for synaptic wiring. *NeuroReport* 13: 795–798 © 2002 Lippincott Williams & Wilkins.

Key words: Cell assembly; Recurrent neural network; Spike-timing-dependent plasticity; Synfire chain; Working memory

INTRODUCTION

In cerebral cortex, a pyramidal-to-pyramidal synapse is potentiated (depressed) if a postsynaptic spike follows (precedes) a presynaptic spike mediated by that synapse [1,2]. In this study, we address how spike-timing-dependent plasticity (STDP) organizes the synaptic connections to achieve persistent activity of low rates in a network of reciprocally connected neurons.

The delay period activity in prefrontal working memory shows low firing rates, typically 20–50 Hz [3–6], which is not currently understood. The role of long-lasting currents, typically persistent Na^+ currents and Ca^{2+}-dependent currents, in the maintenance of the delay period activity has been studied [7,8]. The role of the synaptic connectivity, however, remains to be investigated. Another observation in the monkey prefrontal cortex suggests that some task-related information is retained by the synfire chain, a packet of synchronous spikes traveling through a feed-forward neural network [9–11].

Using Hodgkin–Huxley neurons, we here demonstrate that the self-organization of a recurrent network by STDP results in either a reciprocally connected network showing asynchronous activity or a chain of cell assemblies [12,13], dependent on the timing windows for plasticity. In our model, the asynchronous activity can be retained at low rates (20–30 Hz) not by slow ionic currents, as usually modeled, but solely by the activity regulation induced by STDP. Moreover, this study extends the results of a previous study with integrate-and-fire neurons [13] so that the synfire-like activity can be self-organized for a physiologically realistic range of the timing windows.

MATERIALS AND METHODS

Our model comprises 200 excitatory and 50 inhibitory neurons. STDP is introduced at the recurrent excitatory connections. To elucidate essential roles of STDP, we do not include persistent Na^+ and Ca^{2+}-dependent currents in the excitatory neurons. Thus, the dynamics of each neuron is described by the following Hodgkin–Huxley-like equation:

$$C_m\, dV/dt = -g_L\,(V - E_L) - I_{Na} - I_K - \Sigma_j I_{syn,j} - I_{app} - I_{noise}.$$

Here $C_m = 3.0\,\mu F/cm^2$ (excitatory) or $1.2\,\mu F/cm^2$ (inhibitory), $g_L = 0.14\,mS/cm^2$, and $E_L = -70\,mV$. The kinetics of the spike-generating sodium and potassium currents follow those of the Traub model [14] with $g_{Na} = 100\,mS/cm^2$, $g_K = 40\,mS/cm^2$, $E_{Na} = 45\,mV$, and $E_K = -80\,mV$. The intensity of Gaussian white noise, I_{noise}, is adjusted to give a spontaneous firing of 0.5–1.5 Hz. For glutamatergic ($E_{AMPA} = 0\,mV$) and GABAergic ($E_{GABA} = -70\,mV$) synapses, the synaptic current I_{syn} is described by the first-order kinetics of gating variables [15] with the activation rate $\alpha = 19.8\,ms^{-1}$ and the inactivation rate $\beta = 0.2\,ms^{-1}$. Initial excitatory-to-excitatory connections are all-to-all and are set at a maximum value g_{MAX} (= 0.04 in a unit of g_L). We can adapt random initial weights as well, as far as each neuron receives a sufficiently strong input from other neurons to sustain activity. Other types of connections have the fixed connectivity of 10% and the fixed conductance of 0.04 (AMPA) or 0.05 (GABA) in the same unit.

If the interval Δt from a presynaptic spike to a postsynaptic spike is positive, the conductance of the excitatory-to-excitatory synapse is potentiated as

$g \rightarrow g + g_{MAX}A_p\exp(-\Delta t/\tau_p)$ with $A_p\tau_p = 0.2$ ms. If Δt is negative, the conductance is depressed as $g \rightarrow g - g_{MAX}A_d\exp(-|\Delta t|/\tau_d)$ with $A_d\tau_d = 0.21$ ms. The conductance is kept in the range $0 \leq g \leq g_{MAX}$. To achieve competition among synapses, the area law $A_d\tau_d/A_p\tau_p > 1$ is imposed [16–18]. During learning, we let the network run autonomously without external stimuli. Numerical integration is performed by the fourth-order Runge–Kutta algorithm.

RESULTS

Hereafter, excitatory neurons and excitatory-to-excitatory synapses are simply called neurons and synapses, respectively. In self-organization, the majority of synapses are weakened due to the area law. Except for extremely short τ_p and τ_d (< 10 ms) or for large A_p and A_d (> 0.03), persistent activity of low rates is achieved in simulations. Owing to the activity regulation [17], the postsynaptic firing rate λ_{out} grows more gradually than the presynaptic firing rate, λ_{in}. The rate of persistent activity is approximately given as an intersection of the curve and the line $\lambda_{out} = \lambda_{in}$ (Fig. 1a).

For a timing window with $\tau_d = \tau_p = 10$ ms, a depolarizing step current applied to 30% of excitatory neurons induces persistent activity of 20–30 Hz in the self-organized network (Fig. 1b). A hyperpolarizing step current terminates the activity. The persistent firing state is asynchronous (Fig. 1c),

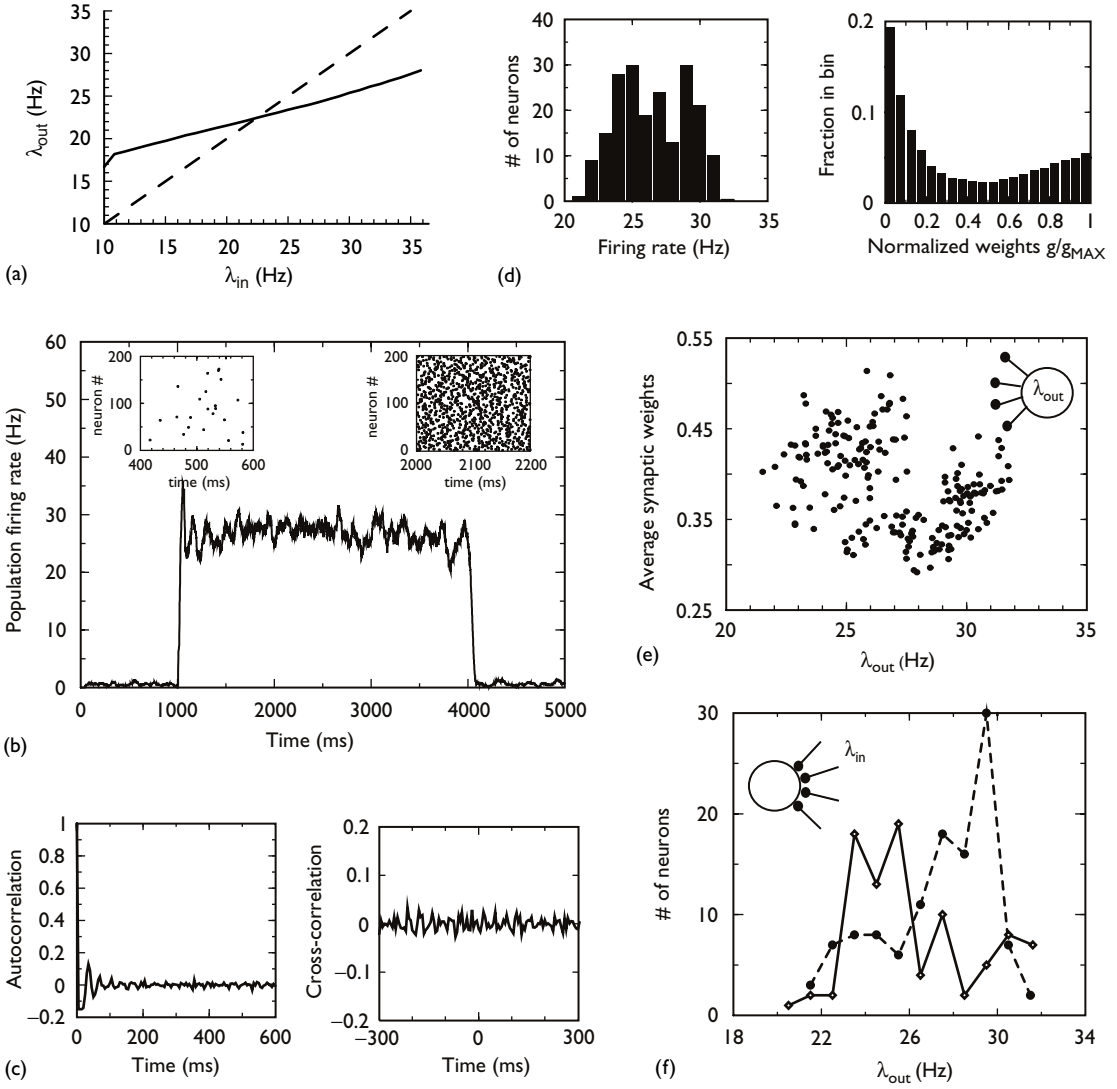

Fig. 1. Asynchronous persistent activity. (**a**) A self-consistency condition on the average rates of input and output spikes determines the rate of persistent activity. The input–output curve was calculated for an integrate-and-fire neuron with the equilibrium synaptic distribution [16], but a similar relationship should hold for a Hodgkin–Huxley-like neuron. (**b**) Bi-stability of the self-organized network. The insets display raster plots of spontaneous firing state and the persistent firing state. (**c**) The spike auto- and cross-correlograms show no characteristic structure. (**d**) The distribution of firing rates (left) and the bimodal distribution of synaptic weights on a neuron (right). (**e**) The relationship between the firing rates and the averaged weights of the out-going fibers. Each dot corresponds to an excitatory neuron. The correlation coefficient is -0.32 ± 0.08, where the error means the s.d. over repeated simulations. (**f**) The distributions of firing rates over the two neural populations classified according to the signature of correlations between presynaptic firing rates and the weights of in-coming excitatory fibers. The solid (dashed) curve is for the neurons with positive (negative) correlations.

involves a broad range of firing rates, and gives a bimodal distribution of synaptic weights on each neuron (Fig. 1d), as in the single-neuron case [16–18,23]. There exists a negative correlation between the firing rate and the average weight of out-going fibers (Fig. 1e), which promotes the activity regulation at the network level. Moreover, STDP enhances (suppresses) the impact of presynaptic spikes on the neurons firing at low (high) rates to stabilize the network activity. In fact, the neurons showing negative (positive) correlations between presynaptic firing rates and the average weights of in-coming fibers tend to fire at high (low) rates (Fig. 1f).

For a timing window with $\tau_d = \tau_p = 20$ ms, synchronized cell assemblies emerge. Initially, the response pattern evoked by a brief stimulus is unstructured (Fig. 2a). In the self-organized network, a synchronized activity can be evoked by a brief stimulus either to neurons in a self-organized layer or to those distributed in the entire network (Fig. 2b). Three assemblies can be defined from the temporal pattern of synchrony. The assembly structure manifests itself in the synaptic connections. On a group-III neuron, for instance, the synapses from a precedent assembly (in this case, II) are strong, while the intra-assembly synapses and those delivered by a subsequent assembly (i.e. I) are weak (Fig. 2c). The weight distribution of the synapses shows sharp bimodal peaks (Fig. 2d) that reflect the chain structure. It is noted that the intra-assembly synaptic connections are essential for propagating a synchronous activity in this network (Fig. 2e), unlike in previous studies for a purely feed-forward model [10,11].

DISCUSSION

The two activity patterns obtained in this study resemble two different forms of memory activity in the monkey prefrontal cortex [3–6,9]. As concerns the synchronous activity, our results are similar to those previously obtained in a network of integrate-and-fire neurons [13], except that cell assemblies emerge in our model for physiologically realistic sizes of the timing window. In both models, there is a difficulty in organizing long chains of assemblies. A sustained synfire activity is most easily realized by the shortest cyclic chain arising from an initially given network. From an initial network with all-to-all connectivity, a chain with three cell assemblies is most likely to emerge (a chain with only two assemblies is forbidden in STDP). Such a short chain, however, is biologically unrealistic. To obtain longer chains, it is necessary to find a more realistic initial connectivity (and to increase the network size). In our model, packets of synchronized spikes are broad compared

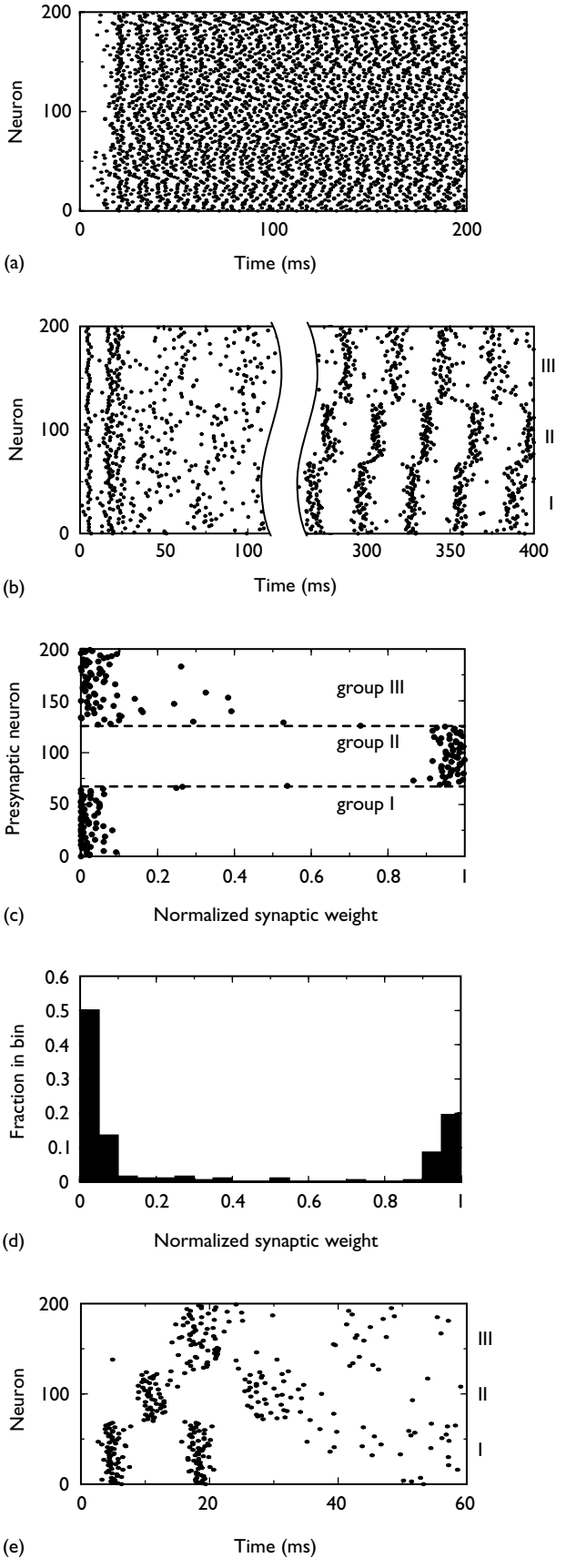

Fig. 2. Near synchronous persistent activity organized by STDP. (**a**) Before learning, activity of an untrained network is not spatio-temporally organized. (**b**) In a trained network, synchronized spike packets are obtained from various initial states. Here, randomly chosen 30% of neurons are activated at an initial time. Excitatory neurons can be rearranged into three cell assemblies (I, II, III). (**c**) The weights of in-coming fibers to a group-III neuron are shown for each presynaptic cell assembly. The weights were normalized by g_{MAX}. Counting the dots in each bin of the normalized weight gives the bimodal distribution shown in (**d**). (**e**) The synchronous activity is unstable if the intra-assembly synaptic connections are eliminated.

with those previously demonstrated in feedforward networks [10,11]. This is presumably because the intra-assembly connections, which make non-negligible contributions to synchronous spike propagation (Fig. 2e), amplify jitters in spike timing. The packets may be narrowed [19] by introducing short-term synaptic depression [20,21].

A remarkable result in asynchronous activity is that low firing rates are obtained by synaptic competition alone without the persistent Na^+ current or the NMDA-receptor-mediated current. As shown in Fig. 1e,f, the present study also revealed some network-level effects on the activity regulation in the entire network. The appearance of asynchronous state for narrow timing windows may be understood from the stochastic synaptic dynamics. In the Fokker–Planck analysis of single neurons, the fluctuations in synaptic weights are proportional to $A_p{}^2\tau_p + A_d{}^2\tau_d$ [16,18,22,23], while the average shifts of weights due to coherent presynaptic spikes are proportional to $A_p\tau_p$. As the timing window is narrowed, keeping $A_p\tau_p$ and $A_d\tau_d$ unchanged, the effects of noise overwhelm those of the coherent input. As synapses become insensitive to the coherent input, a layered neural network is no longer obtained. Also noted is that broad timing windows can sense the weak coherence among temporally separated presynaptic spikes.

For an intermediate range (10–20 ms) of the timing windows, various mixtures of asynchronous and synchronous activities are obtained (results not shown). This seems to imply a continuous transition between the two extremes. This situation is consistent with the following experimental observations: while some prefrontal neuron pairs had significant correlations, others had no significant correlation, even if they showed the delay-period activity related to the same task [3]. It is intriguing to study, from the viewpoints of plasticity, whether and how the delay-period activity is reorganized depending on the functional demand.

CONCLUSIONS

We have shown that spike-timing-dependent plasticity with different timing windows organizes two types of neural networks, one exhibiting asynchronous persistent firing of low rates and one exhibiting a propagating packet of synchronous spikes. Working memory network and 'synfire' chain are different realizations of the single organizing principle and may functionally compensate for one another.

REFERENCES

1. Bi G and Poo M-m. *J Neurosci* **18**, 10464–10472 (1998).
2. Markram H, Lubke J, Frotscher M and Sakmann B. *Science* **275**, 213–215 (1997).
3. Funahashi S and Inoue M. *Cerebral Cortex* **10**, 535–551 (2000).
4. Fuster JM. *The prefrontal cortex: anatomy, physiology, and neuropsychology of the frontal lobe.* New York: Raven; 1997.
5. Goldman-Rakic PS. Toward a circuit model of working memory and the guidance of voluntary motor action. In: Houk JC, Davis JL and Beiser DG, eds. *Models of Information Processing in the Basal Ganglia*. Cambridge: MIT Press; 1995, pp. 131–148.
6. Niki H and Watanabe M. *Brain Res* **105**, 79–88 (1976).
7. Durstewitz D, Seamans JK and Sejnowski TJ. *J Neurophysiol* **83**, 1733–1750 (2000).
8. Lisman JE, Fellous JM and Wang XJ. *Nature Neurosci* **1**, 273–275 (1998).
9. Abeles M, Bergman H, Margalit E and Vaadia E. *J Neurophysiol* **70**, 1629–1638 (1993).
10. Câteau H and Fukai T. *Neural Networks* **14**, 675–685 (2001).
11. Diesmann M, Gewaltig MO and Aertsen A. *Nature* **402**, 529–533 (1999).
12. Brunel N. *J Comput Neurosci* **8**, 183–208 (2000).
13. Horn D, Levy N, Meilijson I and Ruppin E. *Neural Networks* **14**, 815–824 (2001).
14. Traub RD, Wong RKS, Milles R and Michelson H. *J Neurophysiol* **66**, 635–659 (1991).
15. Destexhe A, Mainen ZF and Sejnowski TJ. Kinetic models of synaptic transmission. In: Koch C and Segev I, eds. *Methods in Neural Modeling*. Cambridge: MIT Press; 1998, pp. 1–25.
16. Câteau H, Kitano K and Fukai T. *Neurocomputing* (in press).
17. Song S, Miller KD and Abbott LF. *Nature Neurosci* **3**, 919–926 (2000).
18. van Rossum MC, Bi GQ and Turrigiano GG. *J Neurosci* **20**, 8812–8821 (2000).
19. Fukai T and Kanemura S. *Biol Cybern* **85**, 107–116 (2001).
20. Abbott LF, Varela JA, Sen K and Nelson SB. *Science* **275**, 220–224 (1997).
21. Markram H and Tsodyks M. *Nature* **382**, 807–810 (1996).
22. Kempter R, Gerstner W and van Hemmen JL. *Phys Rev* **E59**, 4498–4514 (1999).
23. Rubin J, Lee DD and Sompolinsky H. *Phys Rev Lett* **86**, 364–367 (2001).

Acknowledgements: The present study was partially supported by Japan Society for Promotion of Science (K.K).